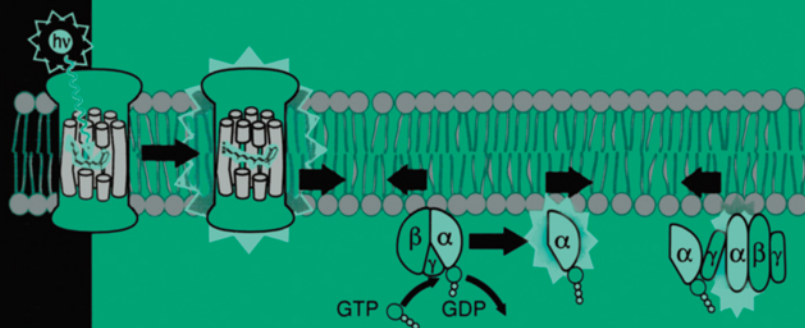


HANDBOOK  
OF  
BIOLOGICAL  
PHYSICS  
SERIES  
EDITOR:  
A.J. HOFF

VOLUME **3**



# Molecular Mechanisms in Visual Transduction

VOLUME EDITORS:

D.G. STAVENGA

W.J. DEGRIP

E.N. PUGH Jr

NORTH-HOLLAND

HANDBOOK

OF

BIOLOGICAL

PHYSICS

VOLUME 3

Molecular Mechanisms  
in Visual Transduction

HANDBOOK  
OF  
BIOLOGICAL  
PHYSICS

---

**Series Editor: A.J. Hoff**

- Volume 1:** Structure and Dynamics of Membranes  
*A: From Cells to Vesicles*  
*B: Generic and Specific Interactions*
- Volume 2:** Transport Processes in Eukaryotic  
and Prokaryotic Organisms
- Volume 3:** Molecular Mechanisms in Visual  
Transduction

HANDBOOK  
OF  
BIOLOGICAL  
PHYSICS  
VOLUME 3

# Molecular Mechanisms in Visual Transduction

*Editors:*

**D.G. Stavenga**

*Department of Neurobiophysics, University of Groningen  
The Netherlands*

**W.J. DeGrip**

*Department of Biochemistry, University of Nijmegen and  
Department of Biophysical Organic Chemistry  
University of Leiden  
The Netherlands*

**E.N. Pugh Jr**

*Department of Ophthalmology and Institute of Neurological Sciences  
University of Pennsylvania, Philadelphia  
USA*



2000

ELSEVIER

Amsterdam - London - New York - Oxford - Paris - Shannon - Tokyo

**ELSEVIER SCIENCE B.V.**  
Sara Burgerhartstraat 25  
P.O. Box 211, 1000 AE Amsterdam, The Netherlands

© 2000 Elsevier Science B.V. All rights reserved.

This work is protected under copyright by Elsevier Science, and the following terms and conditions apply to its use:

**Photocopying**

Single photocopies of single chapters may be made for personal use as allowed by national copyright laws. Permission of the Publisher and payment of a fee is required for all other photocopying, including multiple or systematic copying, copying for advertising or promotional purposes, resale, and all forms of document delivery. Special rates are available for educational institutions that wish to make photocopies for non-profit educational classroom use.

Permissions may be sought directly from Elsevier Science Global Rights Department, PO Box 800, Oxford OX5 1DX, UK; phone: (+44) 1865 843830, fax: (+44) 1865 853333, e-mail: [permissions@elsevier.co.uk](mailto:permissions@elsevier.co.uk). You may also contact Global Rights directly through Elsevier's home page (<http://www.elsevier.nl>), by selecting 'Obtaining Permissions'.

In the USA, users may clear permissions and make payments through the Copyright Clearance Center, Inc., 222 Rosewood Drive, Danvers, MA 01923, USA; phone: (978) 7508400, fax: (978) 7504744, and in the UK through the Copyright Licensing Agency Rapid Clearance Service (CLARCS), 90 Tottenham Court Road, London W1P 0LP, UK; phone: (+44) 207 631 5555; fax: (+44) 207 631 5500. Other countries may have a local reprographic rights agency for payments.

**Derivative Works**

Tables of contents may be reproduced for internal circulation, but permission of Elsevier Science is required for external resale or distribution of such material. Permission of the Publisher is required for all other derivative works, including compilations and translations.

**Electronic Storage or Usage**

Permission of the Publisher is required to store or use electronically any material contained in this work, including any chapter or part of a chapter.

Except as outlined above, no part of this work may be reproduced, stored in a retrieval system or transmitted in any form or by any means, electronic, mechanical, photocopying, recording or otherwise, without prior written permission of the Publisher.

Address permissions requests to: Elsevier Global Rights Department, at the mail, fax and e-mail addresses noted above.

**Notice**

No responsibility is assumed by the Publisher for any injury and/or damage to persons or property as a matter of products liability, negligence or otherwise, or from any use or operation of any methods, products, instructions or ideas contained in the material herein. Because of rapid advances in the medical sciences, in particular, independent verification of diagnoses and drug dosages should be made.

First edition 2000

**Library of Congress Cataloging in Publication Data**

A catalog record from the Library of Congress has been applied for.

ISSN: 1383-8121  
ISBN: 0 444 50102 9

⊗ The paper used in this publication meets the requirements of ANSI/NISO Z39.48-1992 (Permanence of Paper).  
Printed in The Netherlands.

## General Preface

Biological Physics encompasses the study of the processes of life with physical concepts and methods based on the laws of nature, which are assumed to be equally valid for living and dead matter. A multidisciplinary approach brings together elements from biology – knowledge of the problem that is attacked – and from the physical sciences – the techniques and the methodology for solving the problem. In principle, Biological Physics covers the physics of all of biology, including medicine, and therefore its range is extremely broad. There is a need to bring some order to the growing complexity of research in Biological Physics, to present the experimental results obtained in the manifold of its (sub)fields, and their interpretation, in a clear and concise manner. The Handbook of Biological Physics answers this need with a series of interconnected monographs, each devoted to a certain subfield that is covered in depth and with great attention to the clarity of presentation. The Handbook is structured so that interrelations between fields and subfields are made transparent. Areas, in which a concentrated effort might solve a long-standing problem, are identified. Evaluations are presented of the extent to which the application of physical concepts and methodologies (often with considerable effort in terms of personal and material input) have advanced our understanding of the biological process under examination.

Individual volumes of the Handbook are devoted to an entire “system” unless the field is very active or extended (as e.g. for membranes or vision research), in which case the system is broken down into two or more subsystems. The guiding principle in planning the individual volumes is that of going from simple, well-defined concepts and model systems on a molecular and (supra)cellular level, to the highly complex structures and functional mechanisms of living matter. Each volume contains an introduction defining the (sub)field and the contribution of each of the following chapters. Chapters generally end with an overview of areas that need further attention, and provide an outlook into future developments.

The first volume of the Handbook – Structure and Dynamics of Membranes – deals with the morphology of biomembranes and with different aspects of lipid and lipid–protein model membranes (Part A), and with membrane adhesion, membrane fusion and the interaction of biomembranes with polymer networks such as the cytoskeleton (Part B). The second volume – Transport Processes in Eukaryotic and

Prokaryotic Organisms – continues the discussion of biomembranes as barriers between the inside of the cell and the outside world, or between distinct compartments of the cellular inner space, across which a multitude of transport processes occur.

The present volume extends the scope of the previous volumes to the molecular mechanisms of phototransduction in vertebrates and invertebrates. The molecular properties and the primary photoreactions in rhodopsin are treated in depth. The structure and comparative molecular biology of numerous visual pigments are discussed, and the microvillar and ciliary photoreceptors of invertebrates are examined and compared. Furthermore, modeling approaches of the visual processes in vertebrate and insect photoreceptors are extensively reviewed.

Rhodopsin, as one of the best studied G-protein coupled receptors (GPCR), has become a touchstone for research in other areas of signal transduction. We expect, therefore, that the present volume will provide a valuable reference source for workers in these related fields.

#### *Planned volumes*

The “bottom-up” approach adopted for individual volumes of the Handbook, is also the guideline for the entire series. Having started with two volumes treating the molecular and supramolecular structure of the cell, Volume 3 is the first of several volumes on cellular and supracellular systems. Volume 4, to be published early in 2001, is on Neuro-informatics – neural modelling and information processing. The next two planned volumes are on Molecular motors as chemo-mechanical transduction devices, and on Biological electron transport processes. Further planned volumes are:

- Vision – perception, pattern recognition, imaging
- The vestibular system
- Hearing
- The cardio-vascular system, fluid dynamics and chaos
- Electro-reception and magnetic field effects

Further volumes will be added as the need arises.

We hope that the present volume of the Handbook will find an equally warm welcome in the Biological Physics community as the first two volumes, and that those who read these volumes will communicate their criticisms and suggestions for the future development of the project.

Leiden, Fall 2000  
Arnold J. Hoff  
Editor

## Preface to Volume 3 Molecular Mechanisms in Visual Transduction

Visual transduction is presently one of the most intensely studied areas in the field of signal transduction research in biological cells. Because the sense of vision plays a primary role in animal biology, and thus has been subject to long evolutionary development, the molecular and cellular mechanisms underlying vision have a high degree of sensitivity and versatility. The aims of visual transduction research are first to determine which molecules participate, and then to understand how they act in concert to produce the exquisite electrical responses of the photoreceptor cells.

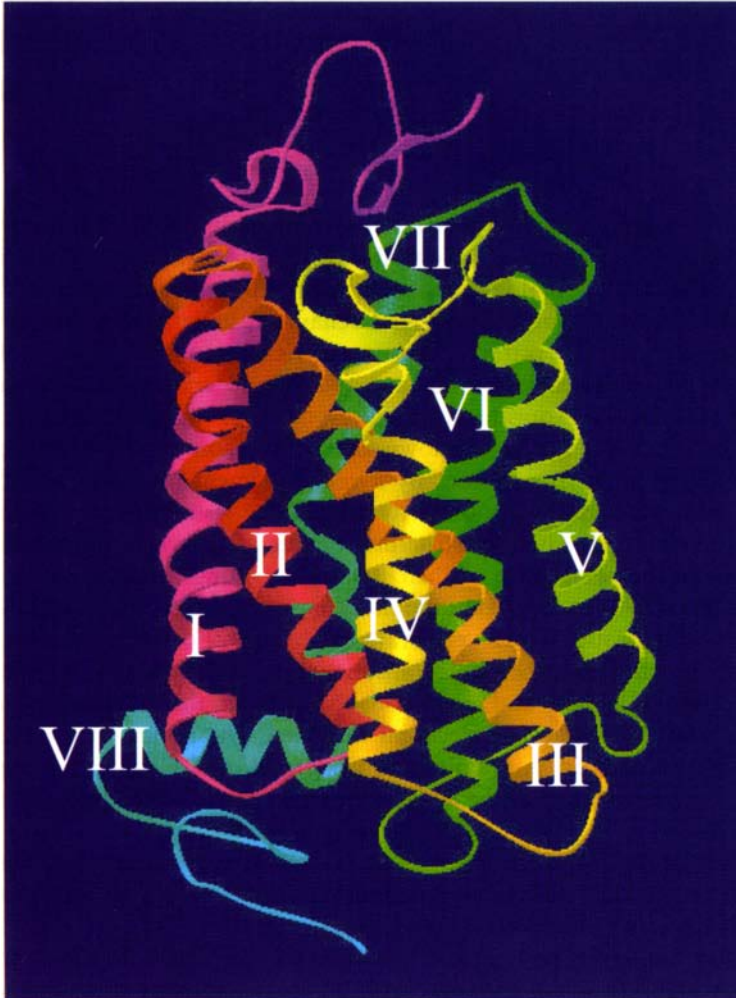
Since the 1940s [1] we have known that rod vision begins with the capture of a quantum of energy, a photon, by a visual pigment molecule, rhodopsin. As the function of photon absorption is to convert the visual pigment molecule into a G-protein activating state, the structural details of the visual pigments must be explained from the perspective of their role in activating their specific G-proteins. Thus, Chapters 1–3 of this Handbook extensively cover the physico-chemical molecular characteristics of the vertebrate rhodopsins. Following photoconversion and G-protein activation, the phototransduction cascade leads to modifications of the population of closed and open ion channels in the photoreceptor plasma membrane, and thereby to the electrical response. The nature of the channels of vertebrate photoreceptors is examined in Chapter 4, and Chapter 5 integrates the present body of knowledge of the activation steps in the cascade into a quantitative framework.

Once the phototransduction cascade is activated, it must be subsequently silenced. The various molecular mechanisms participating in inactivation are treated in Chapters 1–4 and especially Chapter 5.

Molecular biology is now an indispensable tool in signal transduction studies. Numerous vertebrate (Chapter 6) and invertebrate (Chapter 7) visual pigments have been characterized and cloned. The genetics and evolutionary aspects of this great subfamily of G-protein activating receptors are intriguing as they present a natural probe for the intimate relationship between structure and function of the visual pigments. Understanding the spectral characteristics from the molecular composi-

tion can be expected to progress soon from the stage of ordering the visual pigments into spectral classes based on their known primary structure, towards quantitative predictions, with quantum chemical theory.

Although the rhodopsins of vertebrates and invertebrates appear to have much in common (Chapters 6 and 7), their phototransduction processes have diverged. A survey of visual transduction in invertebrates, together with the morphological



Ribbon-structure of bovine rhodopsin based upon the recently published crystal structure [2]. This ribbon-structure was generated at the CMBI, Nijmegen ([www.cmbi.kun.nl](http://www.cmbi.kun.nl)). The N-terminus is at the top, the intracellular surface at the bottom. Note the amphipathic helix conformation of the "8th" helix (bottom) and the remarkable slant of the third transmembrane helix.

differences of the photoreceptor cells, is provided in Chapter 8. Chapter 9 focuses on the fruitfly *Drosophila*, which is not only a classic preparation for the investigation of neural development, but also a rich source for molecular and physiological studies of visual transduction. Finally, Chapter 10 reviews a number of cases where quantitative, modeling approaches have been performed on insect photoreceptors. As is shown in particular in Chapter 5, such an analysis demonstrates that crucial insights into visual transduction can be gained this way.

The relevance of visual pigments and visual signal transduction extends beyond the field of vision. As one of the best studied G-protein coupled receptors (GPCR), rhodopsin and its signaling mechanism have become a prototype for the entire GPCR field. The relative high levels of transduction components in the photoreceptor outer segment has advanced identification and purification of key elements in GPCR transduction, including the G-protein, arrestin, G-P kinase, recoverin, phosducin and RGS-family (Chapter 5). The low-resolution structure of rhodopsin has inspired many protein modelers, seeking a better molecular grip on their favorite GPCR. In this context the very recent publication of the first crystal structure of bovine rhodopsin at better than 3 Å resolution again is a major step forward [2]. The transmembrane  $\alpha$ -helices and the intradiscal (extracellular) connecting loops now have been quite well defined (see figure), allowing reliable modeling of the membrane domain of other GPCRs (Chapter 1).

Hopefully this volume will provide a valuable reference source for a wide audience, not only students and investigators interested in vision, but also for those working in neighbouring areas. Our understanding of visual transduction has now reached a stage where most of the instruments playing in the orchestra are known. We are getting sufficiently familiar with this elegant music, so that its basic themes are becoming well recognizable. But much of its depth and beauty remains to be savored.

## References

1. Hecht, S., Shlaer, S. and Pirenne, M.H. (1942) *J. Gen. Physiol.* **25**, 819–840.
2. Palczewski, K., Kumasaka, T., Hori, T., Behnke, C.A., Motoshima, H., Fox, B.A., LeTrong, I., Teller, D.C., Okada, T., Stenkamp, R.E., Yamamoto, M. and Miyano, M. (2000) *Science* **289**, 739–745.

Doekele G. Stavenga  
Willem J. DeGrip  
Edward N. Pugh Jr

This Page Intentionally Left Blank

## Contents of Volume 3

<i>General Preface</i> . . . . .	v
<i>Preface to Volume 3</i> . . . . .	vii
<i>Contents of Volume 3</i> . . . . .	xi
<i>Contributors to Volume 3</i> . . . . .	xiii
1. W.J. DeGrip and K.J. Rothschild <i>Structure and Mechanism of Vertebrate Visual Pigments</i> . . . . .	1
2. R.A. Mathies and J. Lugtenburg <i>The Primary Photoreaction of Rhodopsin</i> . . . . .	55
3. K.P. Hofmann <i>Late Photoproducts and Signaling States of Bovine Rhodopsin</i> . . . . .	91
4. R.S. Molday and U.B. Kaupp <i>Ion Channels of Vertebrate Photoreceptors</i> . . . . .	143
5. E.N. Pugh Jr and T.D. Lamb <i>Phototransduction in Vertebrate Rods and Cones: Molecular Mechanisms of Amplification, Recovery and Light Adaptation</i> . . . . .	183
6. S. Yokoyama and R. Yokoyama <i>Comparative Molecular Biology of Visual Pigments</i> . . . . .	257
7. W. Gärtner <i>Invertebrate Visual Pigments</i> . . . . .	297
8. E. Nasi, M. del Pilar Gomez and R. Payne <i>Phototransduction Mechanisms in Microvillar and Ciliary Photoreceptors of Invertebrates</i> . . . . .	389
9. B. Minke and R.C. Hardie <i>Genetic Dissection of Drosophila Phototransduction</i> . . . . .	449

10.	D.G. Stavenga, J. Oberwinkler and M. Postma <i>Modeling Primary Visual Processes in Insect Photoreceptors . . . . .</i>	527
	<i>Subject Index . . . . .</i>	575

## Contributors to Volume 3

- W.J. DeGrip*, Department of Biochemistry UMC-160, Institute of Cellular Signaling, University of Nijmegen, P.O. Box 9101, 6500 HB Nijmegen and Department of Biophysical Organic Chemistry, Gorlaeus Lab, University of Leiden, P.O. Box 9502, 2300 RA Leiden, The Netherlands
- M. del Pilar Gomez*, Department of Physiology, Boston University School of Medicine, Boston, MA 02118, USA
- W. Gärtner*, Max-Planck-Institut für Strahlenchemie, Stiftstrasse 34–36, D-45470 Mülheim an der Ruhr, Germany
- R.C. Hardie*, Department of Anatomy, University of Cambridge, Cambridge, CB2 3DY, UK
- K.P. Hofmann*, Institute for Medical Physics and Biophysics, Charité Medical School, Humboldt University, Berlin, Germany
- U.B. Kaupp*, Forschungszentrum Jülich, Institut für Biologische Informationsverarbeitung, 52425 Jülich, Germany
- T.D. Lamb*, Department of Physiology, University of Cambridge, Downing Street, Cambridge CB23EG, UK
- J. Lugtenburg*, Leiden Institute of Chemistry, 2300 RA Leiden, The Netherlands
- R.A. Mathies*, Chemistry Department, University of California, Berkeley, CA 94720, USA
- B. Minke*, Department of Physiology, The Kühne Minerva Center for Studies of Visual Transduction, Hadassah Medical School, The Hebrew University, Jerusalem 91120, Israel
- R.S. Molday*, The University of British Columbia, Department of Biochemistry, 2146 Health Sciences Mall, Vancouver, BC Canada V6T 1Z3
- E. Nasi*, Department of Physiology, Boston University School of Medicine, Boston, MA 02118, USA
- J. Oberwinkler*, Department of Neurobiophysics, University of Groningen, Nijenborgh 4, NL-9747 AG Groningen, The Netherlands

- R. Payne*, Department of Biology, University of Maryland, College Park, MD 20742, USA
- M. Postma*, Department of Neurobiophysics, University of Groningen, Nijenborgh 4, NL-9747 AG Groningen, The Netherlands
- E.N. Pugh Jr*, F.M. Kirby Center for Molecular Ophthalmology, Department of Ophthalmology and Institute of Neurological Sciences, Stellar-Chance Laboratories, University of Pennsylvania, 422 Curie Boulevard, Philadelphia, PA 19104-6069, USA
- K.J. Rothschild*, Department of Physics and Molecular Biophysics Laboratory, 590 Commonwealth Avenue, Boston University, Boston, MA 02215, USA
- D.G. Stavenga*, Department of Neurobiophysics, University of Groningen, Nijenborgh 4, NL-9747 AG Groningen, The Netherlands
- R. Yokoyama*, Department of Physiology, State University of New York Health Science Center at Syracuse, 750 East Adams St., Syracuse, NY 13210, USA
- S. Yokoyama*, Department of Biology, Biological Research Laboratories, Syracuse University, 130 College Place, Syracuse, NY 13244, USA

# Structure and Mechanism of Vertebrate Visual Pigments

W.J. DEGRIP

*Department of Biochemistry,  
University of Nijmegen and  
Department of Biophysical Organic Chemistry,  
University of Leiden*

K.J. ROTHSCHILD

*Department of Physics and  
Molecular Biophysics Laboratory,  
Boston University*

# Contents

1. Introduction	3
1.1. General features of visual pigments	3
1.2. Aim of this review	6
2. Light-triggered steps in rhodopsin activation (photointermediates)	7
2.1. General aspects	7
2.2. Static versus kinetic spectroscopy	7
2.3. Transitions and spectral properties of photointermediates	9
3. Probing structure and mechanism of rhodopsin through electron diffraction, and polarized light, NMR- and ESR-spectroscopy	14
3.1. Electron diffraction and molecular modeling: Rhodopsin's global shape	14
3.2. Polarized light: Relative orientation of structural elements	15
3.3. NMR spectroscopy: High-resolution details	16
3.4. Mutagenesis and ESR studies: Local structure	19
4. Fourier-transform infrared spectroscopy: Conformational changes accompanying receptor activation	22
4.1. General aspects	22
4.2. Early studies: Overall rhodopsin structure	23
4.3. FTIR difference spectroscopy	24
4.4. FTIR characterization of structural changes during photoactivation	25
4.5. Recent progress	28
5. Overview and future perspectives	37
5.1. Overview	37
5.2. Future perspectives	42
References	44

## 1. Introduction

### 1.1. General features of visual pigments

#### 1.1.1. Common structural elements

All visual pigments thus far discovered belong to the super-class of hepta-helical membrane proteins. The bovine rod pigment rhodopsin was the first representative of this superfamily to be recognized. Its amino acid sequence was first elucidated by direct protein sequencing [1,2] and later from its cDNA sequence [3]. This hepta-helical membrane protein family exhibits a broad variety of functional properties, ranging from ion translocation to signal transduction. However, they all share the common structural motif predicted by their amino acid sequences of seven, largely  $\alpha$ -helical, transmembrane segments (TM-domain), which are connected by peptide sequences of variable structure, located outside of the membrane (loops; Fig. 1). The TM-domain folds to present a binding site for a large variety of ligands. In the case of vertebrate visual pigments, the ligand consists of either 11-*cis* retinal (an A<sub>1</sub> retinoid) or 11-*cis* 3,4-dehydroretinal (an A<sub>2</sub> retinoid), which are derived from all-*trans* retinol (vitamin A) or the provitamin  $\beta$ -carotene.

Visual pigments all belong to the G-protein coupled receptors (GPCRs), the largest family of hepta-helical proteins. All GPCRs share common sequence motifs, which are structurally or functionally relevant [4–6]. In addition, there exists a variety of common post-translational modifications including N-glycosylation at Asn residues in the extracellularly located N-terminal region; disulfide bridge formation, linking TM-helix III and the loop between IV and V; and thiopalmitoylation of Cys residues in the intracellularly located C-terminal region [7,8]. The number of thiopalmitoylation sites varies within sub-families of visual pigments, with cone pigments exhibiting zero to one and rod pigments up to two sites [9–11]. Among the G-protein coupled receptors the visual pigments exhibit a unique common structural element: their ligand is covalently attached in the binding site. The linkage consists of a protonated Schiff base with a lysine residue. This configuration is stabilized by a nearby carboxylate anion. This capacity to bind the ligand covalently through a retinylidene Schiff base enables a variety of elegant studies with ligand analogs, that can also be accommodated in the retinal binding pocket [12–14]. The molecular weight of the vertebrate visual pigments varies between 39 and 42 kDa, including ligand and post-translational modifications.

#### 1.1.2. G-protein coupled receptor family (GPCR)

Studies of rhodopsin, a member of the GPCR family, present a unique opportunity both at a basic research level and for pharmacological applications in the treatment of human diseases. The GPCR family comprises a large number of receptors with

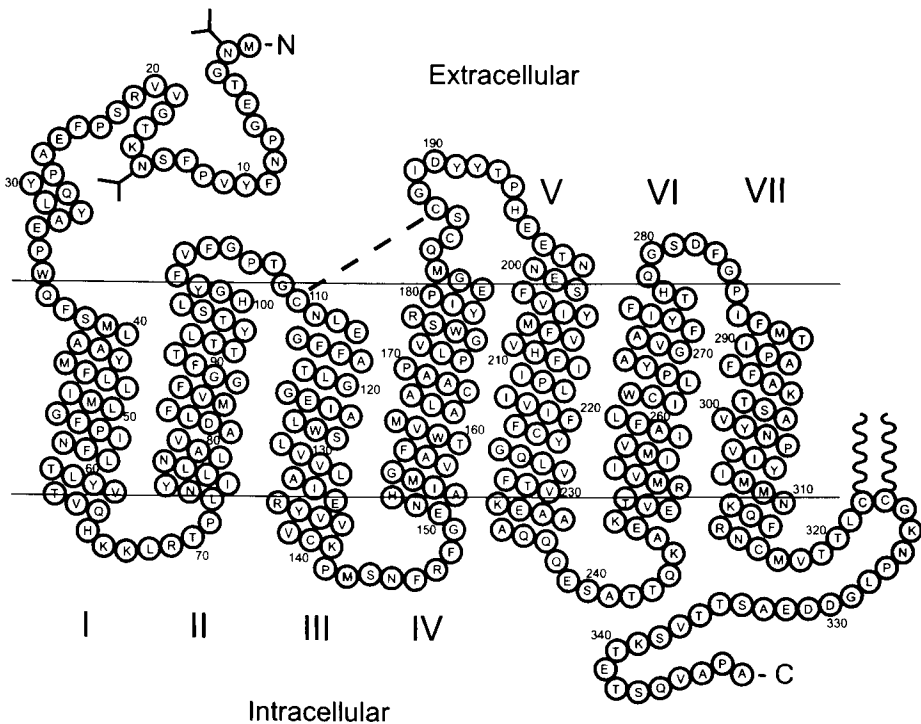


Fig. 1. Amino acid sequence and putative topography of bovine rhodopsin. The arrangement of loops and transmembrane (TM) segments is based on the current state of evidence discussed in the text. Horizontal lines represent the membrane interface. The numbers I–VII indicate the seven TM segments. The corresponding intracellular helical extensions outside the membrane are designated helix A–G, respectively (see text). The following post-translational modifications are indicated: glycan moieties at Asn-2 and Asn-15 in the N-terminal region, disulfide bridge between Cys-110 and Cys-187, and thiopalmitoyl esters at Cys-322 and Cys-323. Numbers indicate protein residue number. Amino acid residues are indicated according to the one-letter convention (A = Ala, etc.). Extracellular corresponds to intradiscal.

hormones, neurotransmitters, peptides, glycoproteins and even small ions as their ligand. Because GPCRs mediate a broad array of important physiological processes they are frequently the target of pharmacological intervention [4,5,15]. The various GPCR sub-classes all contain a variety of isoforms with a different pharmacological profile. Isoform-specific drug design and protein engineering for this receptor family would thus benefit strongly from 3D information on receptor structure and its mode of interaction with its ligands at atomic resolution. Due to their high concentration and specific location in the characteristic ciliary outgrowth of the photoreceptor cell (the outer segment), visual pigments virtually are the only GPCRs, that have thus far been isolated and purified from native sources in sufficient amounts to allow detailed structural studies by biophysical techniques, like crystallography, Fourier transform infrared (FTIR) spectroscopy and NMR spectroscopy. Nevertheless, to

date only a low resolution structure is available for frog and bovine rhodopsin based on electron diffraction and imaging of 2D crystals [16].

GPCRs owe their family name to their common mode of signal transduction; following binding of an activating ligand (agonist) at the extracellular side of the membrane, a conformational change propagates to the intracellular side, which results in binding and activation of a heterotrimeric GTP-binding protein (G-protein). The G-protein consists of three subunits ( $\alpha$ ,  $\beta$  and  $\gamma$ ) for which a large number of partially tissue-specific isoforms exist. Usually the receptor apoprotein, where the ligand site is not occupied (R state), already has some activity ("low-affinity state" or "basal activity" or "constitutive activity"), but this is strongly enhanced upon agonist-binding and subsequent formation of the "high-affinity" or "activated" state (R-A or R\*). In addition, the activity of the receptor or the effect of an agonist can be modulated by other ligands. For instance, partial agonists only activate some of the receptor functions; antagonists counteract the effect of agonists, but do not affect the basal activity, while inverse agonists counteract the effect of agonists and reduce the basal activity as well.

The evolution of GPCRs towards a function in vision required additional specialization [6,8,17,18]. Proper functioning under dim light conditions ("scotopic vision") requires very low noise levels, i.e., a very low basal activity of the receptor. Rapid signal turnover, essential for the necessary fast image processing, requires rapid activation and inactivation kinetics. These two requirements were elegantly realized by occupying the binding site of the receptor in the "dark state" with a photoactive molecule, sensitive to visible light, which acts as an inverse agonist: 11-*cis* retinal. This combination strongly enhances the thermal stability of the protein [19] and very effectively reduces basal receptor activity to such an extent that the rod photoreceptor cell can detect a single photon [20]. Upon absorption of light the 11-*cis*, inverse agonist configuration of the ligand is converted to the all-*trans* configuration, which acts as a full agonist, triggering receptor activation by at least six orders of magnitude (cf. Chapters 3–5 and 8 in this volume). Owing to the inherent high rate of photochemical processes and the fact that ligand-conversion occurs *in situ*, receptor activation does not depend on diffusional processes and is both very efficient and complete within several milliseconds at physiological temperature. In addition, the binding mode of the ligand, a protonated, hence positively charged, Schiff base conjugated with the polyene skeleton, allows modulation of its ground and excited state electronic levels by the electronic charge distribution in the binding site. Hence, through proper selection of relevant residues, the absorbance band of the visual pigment can be shifted over the entire visible range ("spectral tuning") while maintaining the required receptor function (cf. Chapters 6 and 7 in this volume). This is a very important feature, since combining pigments with different spectral sensitivity allows color discrimination (photopic vision). Since the ligand in visual pigments is essential for their spectral properties in the visible region of the spectrum, it often is referred to as the "chromophore".

A major experimental advantage in the study of photosensitive receptors is the ability to synchronously activate an entire population by a light pulse, thereby allowing time-dependent studies. In addition, light activation can be performed at low tem-

peratures, allowing intermediate states to be trapped and their structure characterized. In this way it should be possible to map the structural steps involved in receptor activation at atomic resolution. Thus far, structural details about the pathway for receptor activation are only available for visual pigments and in particular the bovine rod visual pigment rhodopsin. However, it is likely that similar structural studies will become possible for other GPCRs. Recently larger quantities of these proteins can be expressed in heterologous systems, permitting more detailed analysis through mutagenesis and non-radioactive isotope labeling [21–23]. Hence, it is expected that the paradigms evolving for the visual pigment family can soon be tested in other receptors to assess their general value.

### 1.1.3. Vertebrate versus invertebrate visual pigments

As outlined in Chapters 6 and 7 of this volume, vertebrate and invertebrate visual pigments share a common ancestor and thus show a fair degree of sequence and structural homology [24]. On the other hand, the invertebrate pigments use a signal transduction pathway, as discussed in detail in Chapters 8–10 of this volume, which is more closely related to that of other “non-visual” GPCR’s than to that of the vertebrate pigments. In addition, the invertebrate pigments do not release their ligand subsequent to photoactivation, but use instead a reverse photochemical process, which is activated in a different spectral region, in order to return to their “dark state”. These elements are discussed in Chapters 7 and 10 of this volume. Furthermore, their chromophore selection also includes the 3- and 4-hydroxyderivatives of 11-*cis* retinal. Finally, invertebrate pigments become very unstable upon solubilization in detergent solution, which strongly hampers analysis or purification. So far no successful strategies have been reported allowing *heterologous* expression in a functional state. As a consequence, knowledge of structure and structure–function relationships of invertebrate visual pigments is quite limited at present in comparison to their vertebrate counterparts.

### 1.2. Aim of this review

This review will focus on biophysical studies of the structure of vertebrate visual pigments and the conformational changes accompanying photoactivation. Most of these studies have been performed on the bovine rod visual pigment (rhodopsin). While the resulting description probably is applicable to other receptors in a more global sense, details are likely to diverge already between visual pigments (e.g., cone pigments versus rod pigments). It should also be recognized that despite current progress, there are still significant gaps in our knowledge, especially at the level of atomic resolution. Nevertheless, we will attempt to forge the available evidence into a comprehensive and coherent picture of the receptor activation process. As we fill in disputed or blank elements, this will unavoidably include some subjective or provocative interpretations.

The following sections will discuss relevant data obtained by means of UV/visible spectroscopy, solid-state magic-angle spinning NMR spectroscopy, ESR-spectroscopy and FTIR spectroscopy, respectively. Where appropriate, data obtained in mutagenesis studies will also be included. The results will be discussed in

the context of our present knowledge about the rhodopsin structure. Structural data on the invertebrate pigments can be found in Chapter 7 of this volume.

## 2. Light-triggered steps in rhodopsin activation (photointermediates)

### 2.1. General aspects

The first step in the photoactivation of visual pigments, the photo-induced isomerization of the ligand, presents some fascinating photochemistry, that triggers the cascade of structural transitions producing the active receptor conformation. The combination of protein and bound chromophore has evolved in remarkable symbiosis to fine-tune the photoisomerization reaction to near perfection. In model compounds, even in solutions approaching the alleged dielectric conditions in the protein interior, 11-*cis* retinal and derivatives exhibit quantum yields from only 0.05 to 0.15, producing a mixture of stereoisomers with kinetics of several pico-seconds [25,26]. In contrast, photoisomerization in rhodopsin proceeds with an unprecedented quantum yield of 0.67, i.e., every two out of three photons absorbed are effective in activating the ligand and thereby triggering receptor activation [27]. Equally surprising, the reaction is fully stereospecific, producing only the all-*trans* configuration, and is complete within 200 fs [28], making it the fastest photochemical reaction observed to date. Clearly, a special interreactive mechanism must underlie this process. This is discussed in detail in Chapter 2 of this volume.

It was recognized by visual inspection over a century ago that upon light exposure the hue of an isolated frog retina rapidly discolors from red to light-yellow [29,30]. This process has therefore often been referred to as “bleaching”, and more recently and more appropriately as “photolysis”. It has now been established that the light-yellow state represents not only an intermediate step in a complex photolytic sequel but the active receptor state for the visual transduction process, as well. Several decades ago a number of intermediate steps in this photocascade was already identified by their characteristic spectral absorbance bands. This was possible because the photocascade can be fully or partially blocked at characteristic transition temperatures allowing the UV/visible absorption spectrum of intermediates to be obtained by cryospectroscopy [31,32]. The sequence of intermediates discovered in this way is shown in Fig. 2A and represents the classic photocascade. Subsequent rapid progress in kinetic spectroscopy down to femtosecond resolution made it possible to study photoreceptor activation under more physiological conditions. This work confirmed the basics of the classic scheme, but increased its complexity by adding new intermediates (Fig. 2B) (see Section 2.2). As it stands now, the transition steps in the photocascade are well established up to the Meta I intermediate. However, kinetic analyses have not yet yielded a fully consistent picture for the subsequent steps.

### 2.2. Static versus kinetic spectroscopy

The classic picture for the photocascade presented in Fig. 2A was constructed by means of cryospectroscopy, analyzing spectral properties and single transitions

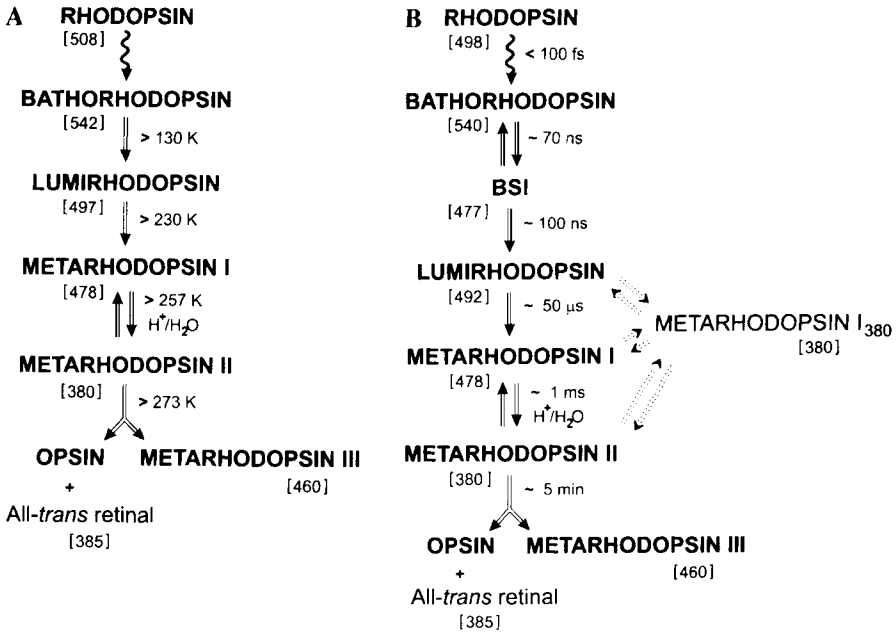


Fig. 2. Intermediates in the rhodopsin photocascade. (A) The photointermediate sequence according to cryospectroscopic studies ("Classic scheme"; see text). Numbers between parenthesis indicate the  $\lambda_{\text{max}}$  of that intermediate below the transition temperature. The transition becomes allowed at the indicated temperature. (B) The photointermediate sequence according to kinetic spectroscopy ("Kinetic scheme", see text). BSI stands for blue-shifted intermediate (see text). Intermediates and transitions, which also have been structurally resolved, are shown in bold and with continuous arrows, respectively. The pathways involving metarhodopsin I<sub>380</sub> need to be further elucidated. Numbers between parenthesis indicate the  $\lambda_{\text{max}}$  of that intermediate at 20°C. The other numbers give approximate half lives of the corresponding intermediate at 20°C.

at specific temperatures [17,31,33–36]. In the scheme obtained [rhodopsin  $\rightsquigarrow$  batho(rhodopsin)  $\rightarrow$  lumi(rhodopsin)  $\rightarrow$  meta(rhodopsin) I  $\leftrightarrow$  meta(rhodopsin) II  $\rightarrow$  meta(rhodopsin) III and opsin] only the first step is light dependent; the subsequent ones are thermodynamically driven. The transition from Meta I  $\rightarrow$  Meta II is accompanied by a large absorbance change from orange to light-yellow. Meta II represents the active receptor, which binds and activates the G-protein (cf. Chapter 2 of this volume). This thermal trapping approach has some disadvantages, however. It basically is restricted to intermediates having increasing enthalpy barriers, thereby obscuring transitions with a significant entropic component, and may be complicated by phase transitions in the lipid matrix or thermal effects on the protein structure [32,33]. Indeed, kinetic spectral studies, performed in the range of room temperature to physiological temperatures with microsecond to picosecond time resolution, have revealed that the photolytic cascade probably is more complicated than suggested by cryospectroscopy, in particular during the Batho  $\rightarrow$  Lumi tran-

sition and in the Meta transitions [33,37]. A putative scheme [33,38–40] is presented in Fig. 2B which is based on global analysis [39]. It should be noted that the currently proposed model may not reflect intermediates which have similar absorbance spectra but different protein structures. It needs to be further established, whether all structural transitions in the protein are accompanied by significant absorbance changes, and vice versa whether all changes in spectral properties necessarily reflect larger structural rearrangements in the protein.

### 2.3. Transitions and spectral properties of photointermediates

#### 2.3.1. Rhodopsin

As mentioned above, the visible spectral properties of vertebrate visual pigments are due to the presence of a ligand or chromophore, 11-*cis* (3,4-dehydro)retinal [17] covalently bound in a protein binding pocket. Binding of dehydroretinal (fairly common in fish and amphibians) results in a red-shifted absorbance spectrum relative to retinal itself (cf. Chapter 6 of this volume). Protein residues in the binding site interact with the chromophore to modulate its electronic properties. In this way a visual pigment can “select” the position of its major absorbance band in the visual spectrum of light (spectral tuning). Taking only 11-*cis* retinal based pigments into account, the following spectral distributions are found: the absorbance band of most rod pigments is centered close to 500 nm [17,18] with some scattered outliers in the range between 480–490 and 505–510 nm (cf. Chapter 6 in this volume). In cone pigments several distinct sub-families can be distinguished, that show relatively high sequence homology and cover specific regions of the visible spectrum [41–47]. The UV/blue sensitive short-wavelength (SW) subgroup covers the range 360–430 nm. The blue-sensitive medium-wavelength (MW1) sub-group is spectrally quite homogeneous: 440–460 nm. The blue/green sensitive medium-wavelength (MW2) sub-group spans a range of 465–510 nm. Finally, the green/red sensitive long-wavelength (LW) sub-group covers the range 508–570 nm. The spectral range of the LW group is quite broad, because the more red-sensitive pigments contain a specific anion-binding site, that under physiological conditions binds chloride, and red-shifts the absorbance spectrum. This red-shift can amount to ca. 30 nm.

At least seven protein residue positions have already been identified which contribute to spectral tuning of visual pigments. Their individual effects are to a large extent additive, in particular within a sub-group. Molecular descriptions of wavelength tuning have been proposed [48–52], though an accurate theoretical explanation will most likely depend on the availability of high resolution structures of the binding site in the various pigment sub-groups. Details and references are given in Chapters 2, 6 and 7 of this volume.

#### 2.3.2. Batho(rhodopsin)

As mentioned before, the formation of this first ground-state product of photoexcitation of visual pigments involves fascinating photochemistry with unprecedented kinetics, as extensively discussed in Chapter 2. This intermediate stores 32–35 kcal/mole of the photon energy [53] in a highly twisted all-*trans* chromophore. Vibra-

tional spectra are comparable at ambient and cryotemperatures [54], suggesting that at this stage only small local changes in protein backbone structure occur, which are most likely largely restricted to protein residues lining the chromophore binding site [55,56]. Evidence has already been presented for "perturbation" of a cysteine, a tryptophan and a tyrosine residue, presumably all located in TM segment VI [57–59] and for participation of Glu113 and Gly121 in TM segment III [60,61]. This is consistent with findings, that the C-3 region of the cyclohexene ring is in close contact with TM VI [62] and upon photoactivation moves closer to TM III [62,63]. In addition, rearrangement of water molecules in the Schiff base region [57,64–67] probably facilitates changes in the protein–chromophore interaction.

The chromophore photoisomerization path is likely to be trapped in Batho in a high-energy intermediate state due to steric interaction with the protein. The contact sites serve to translate the conformational energy, transiently stored in the chromophore, into protein structural changes which eventually uncover latent interaction sites for the G-protein transducin at the intracellular surface. The 9- and 13-methyl groups of the chromophore seem to participate in such energy-transfer. The 9-desmethyl analog of bovine rhodopsin exhibits a significantly altered photocascade, which lacks a well-defined Batho intermediate [36,68] and shows alterations in the subsequent intermediates, as well as perturbed signaling activity [68–70]. The 13-desmethyl analog adopts a chromophore configuration which exhibits a twist different from the native chromophore for the dark-adapted state as well as the Batho intermediate [71–73], but then proceeds to a fairly normal active state [71,74]. Adding a methyl group at the 10-position increases the thermal barrier for decay of Batho [75]. Evidently, chromophore and opsin binding site have been remarkably fine-tuned for optimal energy-transfer [76–79].

### 2.3.3. *Blue-shifted-intermediate (BSI)*

Although low temperature data do not provide a clear indication for the existence of an intermediate between Batho and Lumi in native rhodopsin, evidence for such an intermediate first was found from studies of the rhodopsin analog, 5,6-dihydroisorhodopsin [55,80] and for cyclohexene-ring-modified analogs [81,82]. Subsequent time-resolved studies on native rhodopsin could be interpreted by assuming a Batho  $\leftrightarrow$  BSI equilibrium, with BSI decaying to Lumi [82,83]. This equilibrium is strongly temperature dependent, and at the low temperatures where Batho is trapped in cryostudies, the BSI component would be undetectably small. Hence, structural information on BSI is very limited.

The concept that formation of BSI involves the first stage of relaxation of a steric interaction between the twisted chromophore and the protein, is supported by several observations. First, formation of BSI is much more rapid in the 13-desmethyl rhodopsin analog [84] and BSI may be stabilized at low temperatures in this analog [85]. In addition, the formation rate of BSI is affected by increasing substituent volume at the 9-position of retinal, or at position Gly-121 of rhodopsin [61,86,87], proposed to be located close to the 9-methyl-group [70]. The available evidence suggests that formation of BSI is accompanied by small structural transitions in the protein, which allow repositioning of the C13–C15 section of the

polyene chain [56,84,88–90] and re-orientation of the polyene chain with respect to the ring segment. This latter aspect agrees with a report, that a 6-*S-cis*-locked chromophore which strongly restricts flexibility of the chain relative to the ring segment, does not proceed beyond Batho and thermally reverts to the parent pigment [36,91]. Interestingly, a similar behavior is observed in long-wavelength-sensitive (LWS) cone pigments like the chicken red cone pigment iodopsin [92–94] and enhanced by chloride binding [95]. Binding of a chloride ion to LWS pigments effectuates appreciable red shifts in the absorbance spectrum [96–99], and also induces subtle changes near the C14 position of the chromophore in the Batho state [100]. This could indicate, that binding of chloride to a specific binding site in the second extracellular loop [98,101] increases the thermal barrier for Batho decay by rendering the protein structure near the end of the polyene chain of the chromophore more rigid and/or more compact. Time-resolved spectroscopy, on the other hand, reveals a normal Batho → BSI → Lumi sequence for all cone pigments studied at ambient temperatures [35,96,102–105], except that the lifetime of the Batho intermediate is much shorter, while that of BSI is similar to the corresponding intermediate of bovine rhodopsin. Apparently, Batho decay in cone pigments has a much larger temperature coefficient than in rod pigments. The present evidence suggests that the first structural rearrangements in the protein, together with the initial relaxation of the twisted all-*trans* chromophore occurs during formation of BSI, and that this change relieves a constraint for subsequent formation of Lumi.

#### 2.3.4. *Lumi*(rhodopsin)

Evidence indicates that formation of Lumi involves a major relaxation of the chromophore strain (see [56] and Section 4.4.2) with a small increase in reaction volume (ca. 30 ml/mol) relative to rhodopsin [56,106,107]. The reversal of the sign of the predominant CD band from strongly negative in Batho to slightly negative in Lumi [108–110] along with the re-orientation of the major absorption dipole closer to its orientation in rhodopsin [89,111–113] also reflects this relaxation. Nevertheless, there is no evidence for larger conformational changes at the protein level [58,89,108,114,115], suggesting that these have not yet propagated far from the binding site and are still largely confined to the environment of the chromophore [116]. This agrees with the fact that Lumi can form at low temperature (130 K) [31,117] as well as in extensively dehydrated photoreceptor membrane [66,118–120], conditions which do not allow much conformational flexibility of the protein. This picture of a Lumi intermediate consisting of a largely relaxed chromophore and structural rearrangement of the binding-site which has absorbed most of the stored photon energy also agrees with several other observations [33]. For instance, in contrast to Batho, Lumi is not easily photoconverted back to rhodopsin. Instead, illumination produces a mixture of several *cis*-isomers of retinal [32,115]. Furthermore, in the case of the 10-methyl rhodopsin analog, the Batho intermediate is stable up to a much higher temperature (180 K) and retains all the characteristics of chromophore strain until it decays into Lumi [75].

### 2.3.5. *Meta(rhodopsin) I, II and III*

While a one-step transition from Lumi to Meta I<sub>480</sub> was suggested by low temperature studies on bovine rhodopsin, similar analyses of chicken rhodopsin indicated that the situation is more complex [121]. Time-resolved analyses at ambient up to physiological temperatures also can only be interpreted by assuming a more complex situation [33,38,40,122–124]. Although several schemes have been presented, most require an intermediate absorbing at 380 nm. that is in equilibrium with Lumi and precedes Meta I<sub>480</sub>; it therefore has been dubbed Meta I<sub>380</sub>. Global analyses indicate that Meta I<sub>480</sub> only would be a minor intermediate at temperatures above ambient. Nevertheless, bulkier retinal analogs (10-methyl-, 12-methyl-) stabilize a 480 nm-absorbing intermediate with all characteristics of Meta I<sub>480</sub> up to at least 30°C [75]. This does not really comply with parallel pathways originating from Lumi. Further studies will be needed to clarify the interrelationship between Meta I<sub>480</sub> and Meta I<sub>380</sub> and to determine if these states represent structurally distinct intermediates in the photocycle or rather spectral isoforms of the same global protein conformation, only differing in very local structural elements controlling Schiff base protonation [125].

The Meta I → Meta II transition is the first one that does not proceed under dehydrated conditions [66,118,120,126], and depends on a variety of micro-environmental conditions like pH, surface potential, lipid unsaturation, pressure and lipid-to-protein ratio [114,127–151]. This transition is accompanied by a positive reaction volume of 108 ml/mol, deprotonation of the Schiff base and uptake of a proton from the cytosol [124] (cf. Chapter 3 in this volume), which largely explains the dependence on its micro-environment. Deprotonation and proton uptake can be uncoupled by solubilization in detergents [152]. This slows down the latter process, but in the membrane-bound state deprotonation is the rate-determining step. Hence, the Meta II<sub>a</sub> → Meta II<sub>b</sub> transition has been introduced, representing the deprotonated and the deprotonated, acidified isospectral forms, respectively. Schiff base deprotonation explains the large bathochromic shift (480 → 380 nm) between Meta I<sub>480</sub> and Meta II. All available evidence indicates that Schiff base deprotonation is accompanied by protonation of its counterion Glu-113 [126,153].

Mutation of an essential glutamate residue (E134 in bovine rhodopsin) abolishes external proton uptake [154], but also increases the basal signal transduction activity of the apoprotein (constitutive activity) and the activity induced by free all-*trans* retinal [155–160]. Mutation of several histidine residues, in particular H211, also affects the Meta I ↔ Meta II equilibrium [161,162]. Cone pigments do not clearly exhibit a pH-dependent Meta I ↔ Meta II equilibrium, possibly because of a strong upshift in pK<sub>a</sub> [35,99,163]. They do not have the equivalent of H211, but do contain the equivalent of E134. However, cone pigments have a much higher isoelectric point, and consequently a quite different charge distribution, and, in contrast to rod pigments, a net positive charge at physiological pH [164]. In addition, cone pigments exhibit a much shorter half-life of Meta II [35,99,165–167]. This has been connected to the absence of the glutamate residue at position 122 ([167], however see [99,168]), which is fully conserved only in rod pigments. There is increasing evidence that the surface charge strongly affects the pK<sub>a</sub> of the Meta I ↔ Meta II equilibrium as well

as the rate of Meta II formation [138,147,151,162,169,170]. One attractive mechanism to explain the above-mentioned observations is the existence of (an) H-bonded network(s) in rhodopsin, that act(s) as a structural element as well as helps convey the receptor activation signal from the ligand site to the intracellular membrane surface [171]. Such a network can easily undergo rearrangements through alteration in the internal hydrogen bonding pattern or through proton uptake and re-orientation of bound water molecules and would be expected to be sensitive to surface charge and/or membrane voltage. Several lines of evidence support the presence of such a voltage-sensitive hydrogen-bonding network in bacteriorhodopsin [172–178].

The Meta transitions and their relation to signal transduction are extensively discussed in Chapter 2. Here we will restrict ourselves to structural data. On the basis of volume changes, the formation of Meta II appears to involve the largest conformational change in the photocascade of rhodopsin. This is also suggested by FTIR data (see Section 4.4.4) and surface plasmon resonance studies [179,180]. Ample evidence has been provided for participation of aromatic residues in these conformational rearrangements in the protein [165,181–184]; some of them have been mapped to TM's III and VI [185]. Such changes should serve to expose binding sites for the G-protein transducin at the cytoplasmic segments of the receptor [144,186–188]. In addition to protein conformational changes, several lines of evidence indicate that this structural activity includes the chromophore, even as late as the Meta II step of receptor activation. For instance, chromophore homologs (10-methyl- or 12-methyl-) strongly retard or completely inhibit formation of Meta II [75], while deletions in the cyclohexene ring may abolish Meta II formation [189,190]. In addition, studies of oriented systems provide evidence for a re-orientation of the chromophore during the Meta I  $\rightarrow$  Meta II transition [191,192].

Decay of Meta II into Meta III represents the first slow transition in the photocascade (half life of  $\sim 5$  min at ambient temperature) and is accompanied by a nearly complete loss of signaling activity. The nature of the conformational changes accompanying this transition are not well understood. Although no direct evidence exists, the position of the absorbance band of Meta III (450–460 nm) suggests that it contains an unperturbed protonated Schiff base linkage with retinal. For instance, acid denaturation of rhodopsin generates a product absorbing at ca 445 nm [193,194]. Sulfhydryl activity [195], accessibility of a specific epitope [188] and FTIR analyses [196,197] indicate, that the protein largely refolds upon decay of Meta II into a conformation resembling that of rhodopsin. Regeneration studies demonstrate that Meta III binds 11-*cis* retinal and forms a pigment with spectral properties identical to rhodopsin [194,198]. Such data strongly indicate that the decay of Meta II involves the transfer of all-*trans* retinal from its original binding site to another, possibly non-specific site, along with the partial formation of a protonated Schiff base. Indeed, chemical analysis reveals phospholipids as well as protein amino groups as potential acceptor sites [194], while in Meta II retinal is not in close contact with lipids [199].

This interpretation is difficult to reconcile, however, with reports that Meta III is in equilibrium with Meta II [191,200], and might represent a temporary storage form to replenish Meta II inactivated by phosphorylation and arrestin binding. First of

all, all-*trans* retinal cannot easily re-enter the opsin binding site [201,202]. In addition, it has only recently been established that the addition of all-*trans* retinal enhances the basal signaling activity of opsin [202–206]. This may have previously led to erroneous conclusions as to reformation of an active state (Meta II; 380 absorbance band very similar to all-*trans* retinal [128]) from a Meta III-like state. Upon addition to membranes, retinal easily and randomly forms Schiff bases with available amino groups, that under physiological pH are partially protonated and have absorbance bands peaking in the range 420–470 nm [193,207–209]. Finally, it should be realized that, while Meta III is quite stable *in vitro*, this is not the case *in vivo* where the retinal is transferred to a retinol oxidoreductase and reduced to all-*trans* retinol or vitamin A<sub>1</sub> [210–214]. This would not support a temporary storage function for Meta III. Since FTIR evidence also agrees with a very similar structure for opsin and Meta III (Section 4.4.5), we favor the interpretation that the decay of Meta II into Meta III or opsin releases the retinal from its binding pocket.

### 3. Probing structure and mechanism of rhodopsin through electron diffraction, and polarized light-, NMR- and ESR-spectroscopy

#### 3.1. Electron diffraction and molecular modeling: Rhodopsin's global shape

Almost all high-resolution structural data of proteins have been obtained via X-ray diffraction of suitable 3D-crystals. While over a 1000 structures of soluble proteins have been solved in this way (cf. Protein database at <http://www.rcsb.org/pdb/> or Swiss-Prot database at <http://www.expasy.ch/sprot/sprot-top.html>), very few integral membrane proteins are amenable to such analysis due to difficulties of forming 3D-crystals. Instead, most structures of membrane proteins solved at medium-to-high resolution have been obtained through electron diffraction or imaging of 2D crystals [215–218]. This technique generates a 2D-projection structure, from which, a 3D-structure can be constructed by repeating the analysis at various angles of the crystal relative to the electron beam.

In the case of visual pigments this approach has thus far succeeded in producing a medium resolution (5–10 Å) structure of bovine, frog and squid rhodopsin [16,24,219,220]. Significantly, this work is the first medium resolution structure available for any GPCR and provides the first experimental confirmation for the presence of seven transmembrane  $\alpha$ -helices in this receptor family [16].

Most helices transverse the membrane at an angle which significantly deviates from the membrane normal (Fig. 3), in agreement with the average angle of 35–40° predicted from FTIR analysis of oriented membranes [192,221–223]. It can be estimated that about 50% of the protein mass resides in the membrane, which is in good agreement with earlier neutron diffraction studies [7,224,225]. Combining these projection data with sequence and residue conservation and mutation effects in a large number of GPCR's, Baldwin [226,227] has proposed a general model for the arrangement and orientation of the transmembrane  $\alpha$ -helices in the GPCR 7TM-complex. This model has laid the basis for several refined molecular modeling studies, employing a variety of programs to describe molecular interactions and

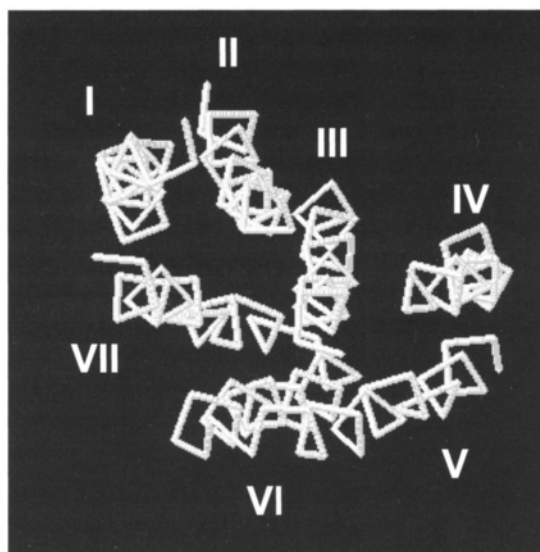


Fig. 3. Orientation of the transmembrane segments of bovine rhodopsin. The data is based on 2D projection structures and adapted from Baldwin [227]. Rhodopsin is viewed from the intracellular side. The numbering of the transmembrane segments corresponds to Fig. 1.

perform energy minimization [13,65,228–231]. However, a more detailed model which reveals atomic resolution information on the position of chromophore and protein residues is still difficult to achieve on the basis of the present structural information. For the time being, data from non-diffraction techniques will be essential to improve current models. For example, all models comply with a negative helicity in the C11–C13 segment of the chromophore, proposed on basis of earlier exciton coupled CD studies [232]. However, recent *ab initio* calculations of CD-spectra support the presence of a positive helicity in this segment of the chromophore ([233], Buss, V. unpublished). These first *ab initio* calculations of CD-spectra seem to be quite reliable, as they also agree with the highly twisted structure proposed by *ab initio* Car-Parinello calculations for the chromophore in Batho [234,235].

### 3.2. Polarized light: Relative orientation of structural elements

Intact rod outer segments can be oriented in a magnetic field due to the stacking of disc photoreceptor membranes in the rod, the intrinsic orientation of  $\alpha$ -helices in rhodopsin and the diamagnetic anisotropy of peptide groups [236]. This has been put to elegant use in early studies with polarized light (Linear Dichroism, LD) [237,238]. First it was determined that the major absorption dipole of the chromophore was oriented nearly parallel to the membrane plane (angle of ca.  $18^\circ$  [239–241]). This is nearly optimal for light absorption in the intact eye, where the incoming light beam runs more or less parallel to the long axis of the photoreceptor